Elgin, S. C. R., Froehner, S. C., Smart, J. E., and Bonner, J. (1971), *Adv. Cell. Mol. Biol. 1,* 1.
Fasman, G. D., Schaffhausen, B., Goldsmith, L., and Adler, A. (1970), *Biochemistry 9,* 2814.
Girod, J. C., Johnson, Jr., W. C., Huntington, S. K., and Maestre, M. F. (1973), *Biochemistry 12,* 5092.
Greenfield, N., and Fasman, G. D. (1969), *Biochemistry 8,* 4108.
Haynes, M., Garrett, R. A., and Gratzer, W. B. (1970), *Biochemistry 9,* 4410.
Hewish, D. R., and Burgoyne, L. A. (1973), *Biochem. Biophys. Res. Commun. 52,* 504.
Hnilica, L. S., and Bess, L. G. (1965), *Anal. Biochem. 12,* 421.
Hooper, J. A., Smith, E. L., Sommer, K. R., and Chalkley, R. (1973), *J. Biol. Chem. 248,* 3275.
Ivanov, V. I., Minchenkova, L. E., Schyolkina, A. K., and Poletayev, A. I. (1973), *Biopolymers 12,* 89.
Johns, E. W., Phillips, D. M. P., Simson, P., and Butler, J. A. V. (1960), *Biochem. J. 77,* 631.
Jordan, C. F., Lerman, L. S., and Venable, J. H., Jr. (1972), *Nature (London), New Biol. 236,* 67.
Maniatis, T., Venable, J. H., Jr., and Lerman, L. S. (1974), *J. Mol. Biol. 84,* 37.
Martinson, H. G., and McCarthy, B. J. (1975), *Biochemistry 14,* 1073.
Marushige, Y., and Marushige, K. (1974), *Biochim. Biophys. Acta 340,* 498.
Olins, A. L., and Olins, D. E. (1974), *Science 183,* 330.
Palau, J. and Dabán, J. R. (1974), *Eur. J. Biochem. 49,* 151.
Panyim, S., and Chalkley, R. (1969a), *Arch. Biochem. Biophys. 130,* 337.
Panyim, S., and Chalkley, R. (1969b), *Biochemistry 8,* 3972.
Panyim, S., Sommer, K. R., and Chalkley, R. (1971), *Biochemistry 10,* 3911.
Patthy, L., Smith, E. L., and Johnson, J. (1973), *J. Biol. Chem. 248,* 6834.
Pinkston, M. F., and Li, H. J. (1974), *Biochemistry 13,* 5227.
Ruiz-Carrillo, A., and Allfrey, V. G. (1973), *Arch. Biochem. Biophys. 154,* 185.
Sadgopal, A., and Bonner, J. (1970), *Biochim. Biophys. Acta 207,* 227.
Sautière, P., Tyron, D., Laine, B., Mizon, J., Ruffin, P., and Biserte, G. (1974), *Eur. J. Biochem. 41,* 563.
Shih, T. Y., and Fasman, G. D. (1970), *J. Mol. Biol. 52,* 125.
Shih, T. Y., and Fasman, G. D. (1971), *Biochemistry 10,* 1675.
Shih, T. Y., and Fasman, G. D. (1972), *Biochemistry 11,* 398.
Šponar, J., Bláha, K., and Štokrová, S. (1973), *Stud. Biophys. 40,* 125.
Van Holde, K. E., Sahasrabuddhe, C. G., and Shaw, B. R. (1974), *Nucleic Acids Res. 1,* 1579.
Wangh, L., Ruiz-Carrillo, A., and Allfrey, V. G. (1972), *Arch. Biochem. Biophys. 150,* 44.
Weintraub, H., and Van Lente, F. (1974), *Proc. Natl. Acad. Sci. U.S.A. 71,* 4249.
Yeoman, L. C., Olson, M. O. J., Sugano, N., Jordan, J. J., Taylor, C. W., Starbuck, W. C., and Busch, H. (1972), *J. Biol. Chem. 247,* 6018.

Localization of the Structural Change Induced in tRNA^{fMet} (*Escherichia coli*) by Acidic pH†

Minou Bina-Stein and Donald M. Crothers*

ABSTRACT: We have compared the molecular mechanism of thermal unfolding for native tRNA^{fMet} (*Escherichia coli*) and the denatured species produced by annealing at pH 4.3. Relaxation kinetic measurements reveal that the transitions assigned to melting of TψC, anticodon, and acceptor stem helices at neutral pH remain essentially unaltered at pH 4.3, but the transition corresponding to coupled melting of tertiary structure and dihydrouridine helix is greatly affected. The T_m of this region is more than 20° higher at pH 4.3 and it has a larger enthalpy of formation than in the native state. The transition dynamics are also considerably changed. In contrast to the native structure, tRNA$^{fMet}_1$ and tRNA$^{fMet}_3$ have similar tertiary structure stabilities at pH 4.3. We conclude that the structural difference between native and acid-denatured forms is localized in the tertiary structure–dihydrouridine helix cooperative interaction region of the molecule.

The structure of tRNA molecules is frequently sensitive to their environment. The earliest examples of this were the denatured forms of tRNA^{Leu} (yeast) and tRNA^{Trp} (*Escherichia coli*) (Lindahl et al., 1966; Gartland and Sueoka, 1966; Lindahl et al., 1967), which are induced by removal of Mg^{2+} or by other changes in environmental conditions. Later, Cole et al. (1972) showed that at reduced ionic strength and without Mg^{2+}, many tRNAs take on an altered form. Furthermore, reduction of pH is also known to change tRNA structure (Bina-Stein and Crothers, 1974). Finally, it is not clear to what extent the influence of crystal form on structure may be responsible for residual disagree-

† From the Department of Chemistry, Yale University, New Haven, Connecticut 06520. *Received March 24, 1975.* This work was supported by a Grant GM 12589 from the National Institutes of Health. D.M.C. holds a Career Development Award (GM 19978) from the same source.

ment about the three-dimensional structure of yeast $tRNA^{Phe}$ (Robertus et al., 1974; Kim et al., 1974).

Assignment of a structural basis for the conformational differences observed in solution has not been straightforward. The problem has been approached using nuclear magnetic resonance (NMR) measurements (Wong et al., 1973; Kearns et al., 1974), enzymatic digestion patterns (Streeck and Zachau, 1971), oligonucleotide binding (Uhlenbeck et al., 1972), and tritium exchange (Webb and Fresco, 1973), with results that are generally informative but not definitive. Our purpose here is to illustrate another strategy for approaching the problem. The principle is simple: we look for changes in the thermal unfolding pattern of the altered form, comparing it with the pattern for the native form. When the structural basis for individual unfolding steps is known for the native structure, disappearance or alteration of one of the steps indicates a modification of the corresponding structural region. If, on the other hand, a particular melting transition is unmodified it is likely that the corresponding structure is still intact, although one must acknowledge the possibility that the altered structure has a new interaction region with thermodynamic and kinetic properties coincidentally identical with those of a region in the native form.

$tRNA^{fMet}$ from *E. coli* provides particularly favorable circumstances for this approach to localizing the structural basis for RNA conformational changes. Combination of proton NMR and relaxation kinetic measurements recently allowed us to specify the molecular mechanism of thermal unfolding of $tRNA^{fMet}_1$ (Crothers et al., 1974). Four steps are involved: first, at lowest temperature, there is simultaneous melting of the dihydrouridine (D) helix plus tertiary interactions, followed by approximately sequential melting of the TψC helix, anticodon helix, and acceptor stem. Wide separation of these transitions is possible only in absence of Mg^{2+}, but our more recent work (A. Stein, to be published) indicates that this is not a serious disadvantage, since addition of Mg^{2+} does not produce any new melting transitions.

As we will report here, $tRNA^{fMet}$ shows altered structure at acidic pH, analogous to the behavior reported earlier for $tRNA^{Tyr}$ (*E. coli*). Relaxation kinetic measurements of the thermal unfolding of $tRNA^{fMet}$ at pH 4.3 show that the last three melting steps change very little from their characteristics at neutral pH, but the first step, corresponding to melting of D helix plus tertiary structure, is grossly altered. This implies that the difference between neutral and acid forms is located in that region of the molecule.

Another advantage of the $tRNA^{fMet}$ system is the slow renaturation of the acid form when neutral pH is restored. This allows us to measure aminoacylation under conditions where the acid form renatures only slowly. From these experiments we conclude that the acid form is either charged much more slowly than the native form, or not charged at all. It is important to note that the presence of Mg^{2+} does *not* prevent tRNA from adopting an altered structure at acidic pH, since $tRNA^{fMet}$ exposed to acid in Mg^{2+} also charges more slowly than native $tRNA^{fMet}$. However, the altered renaturation kinetics when Mg^{2+} was present during annealing at acidic pH indicates that the acid structure formed with Mg^{2+} is not identical with the acid form without Mg^{2+}.

Materials and Methods

$tRNA^{fMet}$ (*E. coli*) containing roughly 60% $tRNA^{fMet}_1$ and 40% $tRNA^{fMet}_3$ was purchased from Miles Laboratories. The acceptor activity of the sample was 1720 ± 35 pmol/A_{260}, indicating high purity. A sample of $tRNA^{fMet}_1$ without S_8–C_{13} cross-link and with $tRNA^{fMet}_3$ removed was obtained from Oak Ridge National Laboratory. Samples were dialyzed first against distilled water, then four times against 100 m*M* EDTA before final dialysis against the measurement buffer.

The *acceptor activity* was determined in an assay system containing 100 m*M* cacodylate buffer (pH 7.0), 2 m*M* ATP, 10 m*M* KCl, 10 m*M* magnesium acetate, and appropriate amounts of $tRNA^{fMet}$, aminoacyl-tRNA synthetase (a crude preparation from *E. coli* K12 generously provided by Dr. David Yang), and [^{14}C]methionine (Schwarz/Mann, specific activity 55.4 Ci/mol). The reaction mixture was incubated for 10 min at 37°, then chilled in an ice bath. A known amount of the mixture was transferred to a 3MM Whatman disk, which was washed in cold trichoroacetic acid, ethanol, and ether, and finally with ether. After drying, the disk was counted in the usual manner in a Packard Model 3320 liquid scintillation counter.

Charging kinetics were measured on tRNA samples dialyzed against appropriate buffers. At various time intervals aliquots were transferred to a filter disk and prepared for counting as described above.

Buffers. Two principal buffers were used in this study. The acidic buffer (buffer I) contained 10 m*M* sodium acetate (pH 4.3), 1 m*M* EDTA, and an appropriate amount of NaCl to bring the sodium ion concentration to 170 m*M*. Buffer II contained 1 m*M* cacodylate buffer (pH 7) instead of acetate, but was otherwise identical. EDTA was omitted from buffer I for the buffer (buffer III) used in the pH-jump experiment.

The *acid form of $tRNA^{fMet}$* was prepared by dialysis of the sample against buffer I, followed by incubation at 70° for 10 min, and quenching in an ice bath.

pH-jump experiments were performed in two ways. Either the pH was raised from 4.3 ± 0.01 to 7.0 ± 0.1 by adding an appropriate amount of a solution containing 10 m*M* sodium cacodylate and 140 m*M* NaOH, or 20 μl of a concentrated solution of the acid form of $tRNA^{fMet}$ at pH 4.3, no Mg^{2+}, was added to 1 ml of a solution containing 100 m*M* sodium cacodylate (pH 7), 10 m*M* KCl, and 10 m*M* magnesium acetate. The latter condition corresponds to the buffer used for measuring aminoacylation of the acid form. Following mixing of the solutions (dead time less than 20 sec), the absorbance change was followed on a Cary 14 spectrophotometer at 260 nm.

pH difference spectra for two samples with identical salt and tRNA concentrations but at pH values of 4.3 and 7.0 were determined by first measuring the (base line) difference spectrum between identical samples at pH 4.3. The pH of one sample was raised to 7.0 as described for pH-jump experiments, and an identical volume of pH 4.3 buffer was added to the other sample to compensate for tRNA dilution. The new increase or decrease in absorbance relative to the base line was then measured as a function of wavelength on the Cary 14.

Molecular weight measurements utilized a Spinco Model E analytical ultracentrifuge equipped with uv optics and a photoelectric scanner. All runs were made in a 12-mm Epon double sector cell at a concentration of about 0.6 A_{260}/ml in buffer I at 10°.

Melting curves were measured on a Cary 14 spectrophotometer, with cell compartment thermostated at 25°. Water-jacketed 1-cm spectrophotometer cells (Helma QS

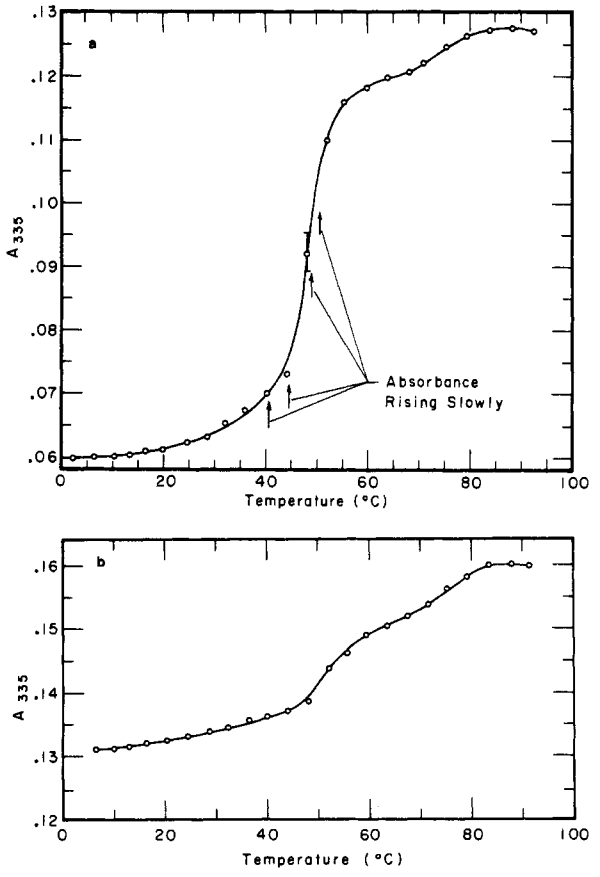

FIGURE 1: (a) Melting curve of tRNA^{fMet} (*E. coli*) at pH 4.3 (0.17 *M* Na^+) measured at 335 nm. The sample had no prior heat treatment. Slow absorbance drift was observed beginning at 40°. (b) Melting curve of tRNA^{fMet} at pH 4.3 (0.17 *M* Na^+) at 335 nm. The sample was heated for 10 min at 70° prior to determination of the transition curve, which was found to be reversible on cooling.

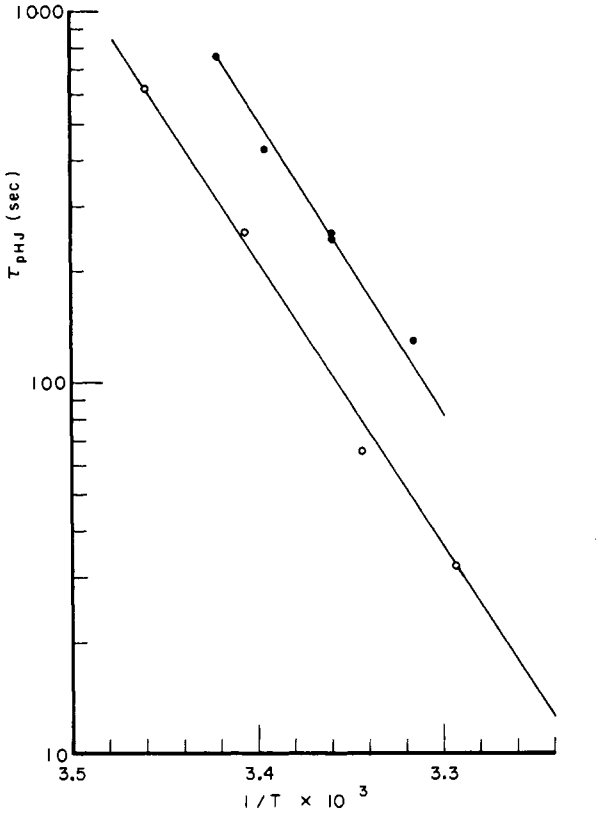

FIGURE 2: Semilogarithmic plot of the relaxation time obtained following a change of pH, from 4.3 to 7, for a sample of tRNA^{fMet} annealed at pH 4.3. (○) Measurements without Mg^{2+}; (●) experiments in which Mg^{2+} was present at pH 7.0. The slope of the semilog plot vs. reciprocal temperature yields an Arrhenius activation energy of 38 ± 3 kcal/mol.

160) were thermostated with another circulating bath. Melting curves were recorded using the 0–0.1 absorbance slidewire, and T_m was taken as the temperature at which the absorbance had risen half-way between its initial and final values.

Temperature-jump measurements were carried out on the instrument previously described (Crothers, 1971). At lower temperatures a temperature jump of 3.7° was achieved by discharge through the cell of 20 kV on a 0.05 μF capacitor. In order to avoid cavitation at high temperatures, the temperature jump size was reduced by using progressively smaller high voltages.

Each relaxation signal ΔA is characterized by a set of exponential decay time constants, called the relaxation times τ_i, and the associated magnitudes of the signal change, called the relaxation amplitudes ΔA_i:

$$\Delta A = \sum_i \Delta A_i \exp(-t/\tau_i)$$

Several relaxation times were observed, depending on the temperature. When the relaxations were well separated on the time axis, each was analyzed as a simple exponential. If, however, two relaxations differed in time constant by only a factor 2 to 10, they were separated graphically. The longer relaxation time was determined first, and its amplitude was subtracted from the total effect to yield the relaxation time and amplitude of the faster effect. It is important to realize that there is considerable uncertainty in coupled relaxation times and amplitudes determined by this method.

Amplitude data were analyzed by plotting $\Delta A_i/\Delta T$ vs. the average of initial and final jump temperatures. The result is a differential melting curve whose width is determined by the apparent transition enthalpy ΔH (Gralla and Crothers, 1973; Crothers et al., 1974).

Results

(*a*) *Equilibrium Melting Curves.* The melting curve of tRNA^{fMet} at 335 nm and pH 4.3 is, unlike tRNA^{Tyr} (Bina-Stein and Crothers, 1974), nearly indistinguishable from that measured at neutral pH (Cole et al., 1972). Both the shape and hyperchromicity of the transitions at 335 and 260 nm are the same as measured under neutral pH conditions (Figure 1). However, considerable upward drift of the 335-nm absorbance was observed between 40 and 55° (Figure 1), reaching equilibrium only after more than 2 hr. When the sample was cooled stepwise, the melting curve was observed to be irreversible. We therefore treated a sample at pH 4.3 for 10 min at 70° prior to melting, and found the fully reversible melting curve shown in Figure 1b. The prior heat treatment greatly alters the melting curve at 335 nm, but has little effect on the 260-nm transition. The transition curve at 335 nm is still biphasic, but the hyperchromicity of the first transition is considerably reduced; the hyperchromicity of the second transition is essentially unchanged by prior heat treatment (Figure 1).

(*b*) *pH-Jump Experiments.* We performed pH-jump experiments (Bina-Stein and Crothers, 1974) on the heat-treated acid form of tRNA^{fMet} in order to observe the ki-

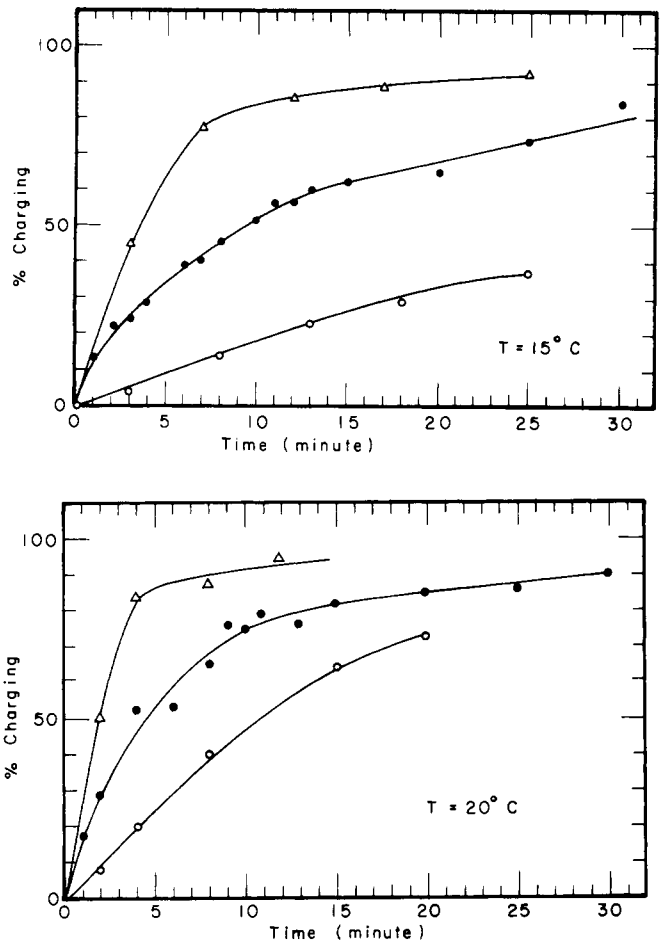

FIGURE 3: Charging kinetics of native and acid forms of $tRNA^{fMet}$ (△) Charging of the native form; (○) charging of $tRNA^{fMet}$ annealed at pH 4.3 without Mg^{2+}, and added to the charging assay mixture at time $t = 0$. (●) charging of $tRNA^{fMet}$ annealed at pH 4.3 with 0.3 mM Mg^{2+}. Data for two temperatures are shown, 15° (upper) and 20° (lower).

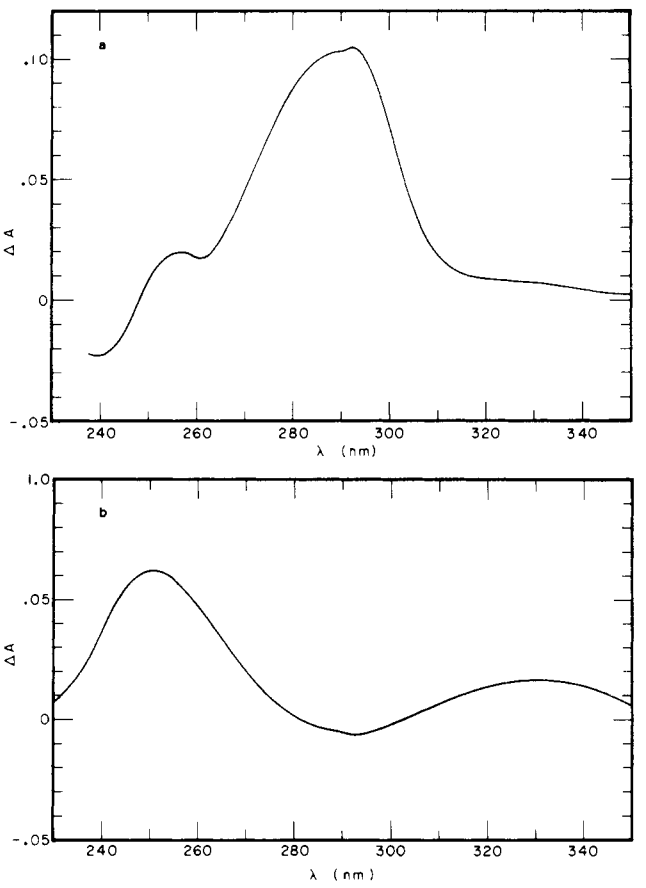

FIGURE 4: Difference spectra for $tRNA^{fMet}$. (a) $tRNA^{fMet}$ annealed at pH 4.3 (sample) − $tRNA^{fMet}$ annealed at pH 7 (reference). Concentration, 1.3 A_{260}/ml. (b) $tRNA^{fMet}$ annealed at pH 4.3 (sample) − $tRNA^{fMet}$ dialyzed to pH 4.3 but not heated (reference). Concentration 1.3 A_{260}/ml.

netics of reconversion to the native form. Rates were measured in the absence or presence of Mg^{2+}. In the former case NaOH was added to raise the pH from 4.3 to 7, and in the latter a concentrated acid-form tRNA sample was diluted into a magnesium-containing solution with the composition of the charging assay buffer (see Materials and Methods). Exponential decay times for the conversion, observed spectrophotometrically, are shown in Figure 2. The time constant when Mg^{2+} is present at neutral pH is about twice as long as when Mg^{2+} is absent, but the activation energies are very similar in the two cases (38 ± 3 kcal/mol). We emphasize that Mg^{2+} was *not* present while the tRNA sample was heat treated at acid pH in these experiments.

(*c*) *Charging Kinetics.* From the pH-jump experiments we infer that the conversion of the heated acid form to the native structure is very slow at low temperature. This slow reconversion made it possible to test the chargeability of the acid form. Figure 3 shows that the rate of its charging is much slower than for the native form. Quantitative comparison indicates that charging occurs at the rate expected for renaturation. For example, at 20°, a fraction $1/e$ remains uncharged at about 900 sec, closely comparable to the optically observed renaturation time constant in the presence of Mg^{2+}. Hence the acid form is either charged much more slowly than the native structure, or it may not be charged at all. In either case, the structural difference induced by low pH is evidently sufficiently large to interfere with tRNA function.

Figure 3 also shows the effect on charging kinetics when Mg^{2+} was present during the acid heat treatment. Charging is faster than when no Mg^{2+} was added at that stage, but not as rapid as for the native form. (All of the charging reactions, of course, occur in the presence of Mg^{2+}). Since charging is not equivalent for an acid + Mg^{2+} heat-treated tRNA and the native tRNA structure, we are forced to conclude that even in the presence of 0.3 mM Mg^{2+}, low pH induces a structural alteration in tRNA. The structure, however, is different from that produced when Mg^{2+} is absent during heat treatment at pH 4.3, since the two charging rates are different.

At higher temperatures the renaturation rate is rapid enough so that the charging rates of acid and native forms are nearly equal. In the usual 10-min incubation at 37°, acceptor activities were 1735 ± 35 mol/A_{260} and 1720 ± 35 pmol/A_{260} for acid and neutral forms, respectively. Hence this particular denatured form is sufficiently labile not to be detected under the usual assay conditions. It is worth noting that the data in Figure 1 indicate that the native form at pH 4.3 is kinetically more stable than the acid form at neutral pH. At pH 4.3, temperatures above 40° are required before conversion to the acid form can be detected from drift in the 335-nm absorbance.

(*d*) *Equilibrium Sedimentation.* Loss of acceptor activity due to aggregation has been reported for a number of

Table I: Comparison of Thermodynamic and Kinetic Properties of Melting Transitions Observed for Native and Acid Forms of tRNA^{fMet}.

tRNA^{fMet} (Buffer I), "Heated acid form"						tRNA$^{fMet}_1$, pH 7 (Crothers et al., 1974), "Native" neutral structure					
Transition	Structural Region	T_m(°C)	τ_{max} (msec)	ΔH (kcal/mol)	E_a (kcal/mol)	Transition	Structural Region	T_m(°C)	τ_{max} (msec)	ΔH (kcal/mol)	E_a (kcal/mol)
1, 2	"Altered structure"	67	90	80		1 (fMet 3)	DHU helix +	30		30	–
						2 (fMet 1)	"tertiary interaction"	46 ± 1	7.0	52 ± 5	50
3	T ψ C arm	59 ± 3	0.013	53 ± 10	47 ± 10	3	T ψ C arm	61 ± 2	0.013	54 ± 10	55
4	Anticodon arm	71 ± 2	0.050	64 ± 4	43 ± 10	4	Anticodon arm	70 ± 10	0.08	58 ± 15	49
5	Acceptor stem	74 ± 3	1.0	64 ± 4	65 ± 10	5	Acceptor stem	77 ± 2	1.3	70 ± 10	62

tRNA species (Schleich and Goldstein, 1964; Söll et al., 1967; Hampel et al., 1971; Adams and Zachau, 1968; Yang et al., 1972). To determine whether the heated acid form of tRNA^{fMet} is a dimer or other aggregate, we determined the molecular weight by sedimentation equilibrium. According to Casassa and Eisenberg (1964), the molecular weight M_2 of a high molecular weight species in a multicomponent mixture is given by

$$M_2 = \left(\frac{2RT}{(\partial\rho/\partial c_2)_\mu}\right)\frac{d \ln c_2}{dx^2}$$

where c_2 is the concentration, x the distance from the axis of rotation, and R and T have their usual meaning. The factor $(\partial\rho/\partial c_2)_\mu$, the density increment due to addition of c_2 at constant chemical potential of the dialyzable components, has not been directly determined for tRNA. Therefore, we use instead a value calculated from our earlier measurements on tRNA^{Tyr} (Yang et al., 1972) under comparable (but not identical) ionic conditions, $(\partial\rho/\partial c_2)_\mu = 0.409$. Sedimentation equilibrium studies at 10° and 17980 rpm (buffer I, pH 4.3) yielded a molecular weight for the acid form of 2.81×10^4, in close agreement with the value 2.86 ± 10^4 calculated for the sodium salt from the known sequence. Hence the heated acid form is monomeric.

(*e*) *Difference Spectra.* Figure 4a shows the difference spectrum between the acid form (at pH 4.3) in the sample compartment with an identical concentration of tRNA^{fMet} at pH 7 in the reference beam. The acid form is hyperchromic relative to the neutral form, with a differential maximum around 290 nm and a secondary maximum at 258 nm. Protonation of cytidine yields a differential maximum at 290 nm, and is probably responsible for the major spectral difference between neutral and acid forms (Bina-Stein and Crothers, 1974). Figure 4b shows the spectral difference between the heated acid form at pH 4.3 (sample) and the metastable native form also at pH 4.3 (reference). Conversion to the acid form at pH 4.3 causes an increase in absorbance, with differential maxima at 250 and 330 nm.

(*f*) *Relaxation Kinetics.* The experiments reported so far establish that tRNA^{fMet} takes on an altered conformation when annealed at pH 4.3, but they do not provide any information on the underlying molecular details. The relaxation kinetic experiments were designed to compare the melting of the acid form of tRNA^{fMet} with the previously reported results for the native form at neutral pH (Crothers et al., 1974). Three transitions (3, 4, and 5) were found to be virtually unaltered by the change in pH from 7 to 4.3. Differential melting curves for these are shown in Figure 5, and

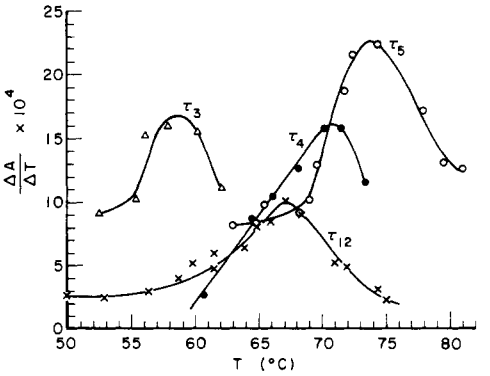

FIGURE 5: Differential melting curves for the relaxation effects 12, 3, 4, and 5 found for tRNA^{fMet} annealed and measured at pH 4.3, 0.17 *M* Na^+. The transitions are assigned to melting of TψC helix, "wrong structure", anticodon helix, and acceptor stem in order of increasing T_m.

the relaxation times are plotted as functions of thermodynamic and kinetic properties for melting of the native and acid forms. (Note that for convenience the numbering system for transitions adopted in our earlier paper (Crothers et al., 1974) has been retained here, even though the numbers do not correspond to the order or number of transitions observed in the present case.) It is evident from the results collected in Table I that the characteristics of transitions 3, 4, and 5 are very similar in the native and acid forms. The T_m values are lower by an average of 2° in the acid form which can be accounted for by the lower pH, and the transition rates are also nearly the same in acid and native states.

The major change in thermal unfolding behavior when tRNA^{fMet} is annealed at low pH is in the transition labeled 12 (Figures 5 and 6). This melting step replaces the separate transitions 1 and 2 seen in tRNA$^{fMet}_3$ and tRNA$^{fMet}_1$, respectively (Crothers et al., 1974). In the Miles sample of mixed isoacceptors 1 and 3 at acid pH, only one transition, τ_{12} (Figure 5), could be resolved in addition to the effects 3, 4, and 5; the same transition was found in a sample of purified tRNA$^{fMet}_1$ (lacking S_8–C_{13} cross-link). Therefore the two separate transitions 1 and 2 are replaced at acid pH by a single transition, with T_m increased to 67° from 30° and 46°. The maximum value of the relaxation time (at the lowest temperatures of observation) was about 90 msec (Figure 6), compared with 3 and 7 msec for τ_1 and τ_2. Finally, the measured enthalpy is 80 kcal/mol, compared to 30 and 52 kcal/mol for transitions 1 and 2, respectively. Hence it is evident that the structural interaction region which becomes unbonded in transition 2 (tRNA$^{fMet}_1$) or transition 1

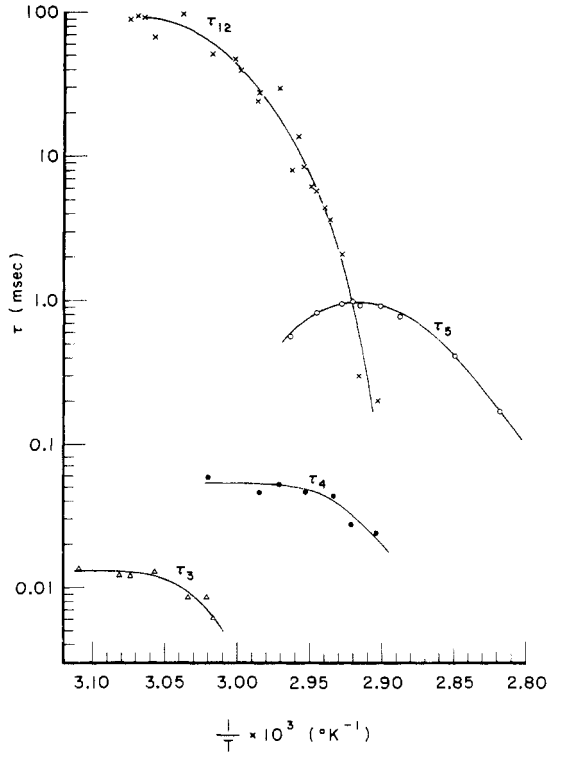

FIGURE 6: Variation of relaxation times 12, 3, 4, and 5 with reciprocal temperature; conditions as in Figure 5.

($tRNA^{fMet}_3$) is substantially altered in the acid form; furthermore, the phenomenon cannot be ascribed to material containing an S_8–C_{13} cross-link. An alteration is implied by the change in thermodynamic and kinetic parameters, and simple protonation is ruled out as the source of the change by the slow rate and large activation energy of reconversion to the native state. We conclude that in the acid form the dihydrouridine helix–tertiary interaction region has a substantially altered structure.

Discussion

The results reported here show that the dihydrouridine helix–tertiary structure region of $tRNA^{fMet}$ is altered by annealing at low pH. The new structure has a higher T_m and greater enthalpy of stabilization than the neutral pH tertiary structure. We infer from the results that the anticodon helix, TψC helix, and acceptor stem helix are most probably unaltered at low pH, although we cannot definitely exclude replacement of one or more of those by an altered helix with stability and dynamics coincidentally identical with a helix present in the neutral form.

The identification of the tertiary structure–dihydrouridine helix as a labile region subject to polymorphism parallels recent models which implicate the same region in the denatured structure of $tRNA^{Leu}$ (Uhlenbeck et al., 1972; Wong et al., 1973). It will be of particular interest to observe the extent of variation in that region as further three-dimensional structures are obtained for tRNA, especially if changes are observed under different crystallization conditions. Structural changes dependent on pH are known in protein crystallography (Vandlen and Tulinsky, 1973; Mavridis et al., 1974), and they can be inferred to occur in other RNAs from the hysteresis observed in acid–base titrations of RNA (Revzin et al., 1973).

Our results cannot, of course, specify the nature of the structural change in the tertiary structure–dihydrouridine helix region, but they provide a few observations that bear on that question. First, since the striking difference between $tRNA^{fMet}_1$ and $tRNA^{fMet}_2$ in tertiary structure stability disappears in the acid form, the m^7G at residue 47 no longer plays a special role in stabilizing the tertiary structure. Second, we found that the TψC helix could melt *before* the "tertiary" structure in the acid form. We have not found this to occur in the native structure. For example, when Mg^{2+} is added to stabilize the tertiary structure of $tRNA^{fMet}$ at neutral pH, the TψC helix T_m begins to increase when it would otherwise be surpassed by the tertiary structure T_m (A. Stein, to be published). The decoupled melting observed in the acid form could mean that tertiary interactions in that state do not involve bonding to the TψC helix or loop. Chemical modification experiments as a function of pH (which is a neglected but potentially important variable in such studies) might help clarify this question.

References

Adams, A., and Zachau, H. G. (1968), *Eur. J. Biochem. 5,* 556–558.

Bina-Stein, M., and Crothers D. M. (1974), *Biochemistry 13,* 2771–2775.

Casassa, E. F., and Eisenberg, H. (1964), *Adv. Protein Chem. 19,* 287–395.

Cole, P. E., Yang, S. K., and Crothers, D. M. (1972), *Biochemistry 11,* 4358–4368.

Crothers, D. M. (1971), *Proc. Nucleic Acid Res. 2,* 369–388.

Crothers, D. M., Cole, P. E., Hilbers, C. W., and Shulman, R. G. (1974), *J. Mol. Biol. 87,* 63–88.

Gartland, W. J., and Sueoka, N. (1966), *Proc. Natl. Acad. Sci. U.S.A. 55,* 948–956.

Gralla, J., and Crothers, D. M. (1973), *J. Mol. Biol. 78,* 301–319.

Hampel, A., Cherayil, J., and Bock, R. M. (1971), *Biochim. Biophys. Acta 228,* 482–491.

Kearns, D. R., Wong, Y. P., Hawkins, E., and Chang, S. H. (1974), *Nature (London) 247,* 541–543.

Kim, S. H., Suddath, F. L., Quigley, G. J., McPherson, A., Sussman, J. L., Wang, A. H. J., Seeman, N. C., and Rich, A. (1974), *Science 185,* 435–439.

Lindahl, T., Adams, A., and Fresco, J. R. (1966), *Proc. Natl. Acad. Sci. U.S.A. 55,* 941–947.

Lindahl, T., Adams, A., Gerock, M., and Fresco, J. R. (1967), *Proc. Natl. Acad. Sci. U.S.A. 57,* 178–185.

Mavridis, A., Tulinsky, A., and Liebman, M. N. (1974), *Biochemistry 13,* 3661–3666.

Revzin, A., Neuman, E., and Katchalsky, A. (1973), *J. Mol. Biol. 79,* 95–114.

Robertus, J. D., Ladner, J. E., Finch, J. T., Rhodes, D., Brown, R. S., Clark, B. F. C., and Klug, A. (1974), *Nature (London) 250,* 546–551.

Schleich, T., and Goldstein, J. (1964), *Proc. Natl. Acad. Sci. U.S.A. 52,* 744–749.

Söll, D. G., Cherayil, J. D., and Bock, R. M. (1967), *J. Mol. Biol. 29,* 97–112.

Streeck, R. E., and Zachau, H. G. (1971), *FEBS Lett. 13,* 329–34.

Uhlenbeck, O., Chirikjian, J. G., and Fresco, J. R. (1972), *Fed. Proc., Fed. Am. Soc. Exp. Biol. 31,* 422.

Vandlen, R. L., and Tulinsky, A. (1973), *Biochemistry 12,*

4193-4200.
Webb, P., and Fresco, J. R. (1973), *J. Mol. Biol. 74,* 387-402.
Wong, Y. P., Kearns, D. R., Shulman, R. G., Yamane, T., Chang, S., Chrikjian, J. G., and Fresco, J. R. (1973), *J. Mol. Biol. 74,* 403-406.
Yang, S. K., Söll, D. G., and Crothers, D. M. (1972), *Biochemistry 11,* 2311-2320.

Infrared Linear Dichroism Investigations of Deoxyribonucleic Acid Complexes with Poly(L-arginine) and Poly(L-lysine)†

J. Liquier, M. Pinot-Lafaix, E. Taillandier, and J. Brahms*

ABSTRACT: Complexes between DNAs from various sources and poly(L-lysine) and poly(L-arginine) were studied by means of infrared linear dichroism. The measurements of dichroic ratios allowed us to determine the orientation of the phosphate group of DNA in the complexes with basic polypeptides. At high relative humidities (higher than 90%, B form), the bisector of the ∠OPO in the complexes forms an angle with respect to the helical axis which has a value lower by about 4° than in the corresponding DNA sample. This change of orientation of the phosphate group of DNA indicates a modification of the B form upon binding of polylysine or polyarginine. The structural transitions B → A and B → C measured as a function of relative humidities were not affected by formation of complexes with both basic polypeptides. Similar results were obtained for complexes prepared by direct mixing or by salt gradient dialysis. The presence of A and C forms was observed in complexes of DNA with poly(L-lysine) and poly(L-arginine) at lower relative humidity. Thus, the conformational flexibility of DNA in complexes with polylysine and polyarginine is not changed despite a substantial increase in the T_m (melting temperature). These results are considered as a model for the understanding of interactions between DNA and histones and particularly of the binding of the N-terminal fragment, lysine or arginine rich.

Deoxyribonucleic acid exists in the nuclei of higher organisms in the form of complex structures associated with proteins. The histones are basic proteins which are found in nuclei tightly bound to DNA and which appear to stabilize the condensed structure of eukaryotic DNA (Pardon and Wilkins, 1972). Detailed knowledge of the structural properties of these complexes might provide a basis for the understanding of the mechanism of function of eukaryotic nuclei; in particular, one may be able to understand the regulation of transcription (Paul, 1972; Sutton, 1972; Elgin et al., 1971). It is evident that the complexity of these DNA-protein complexes and their interactions with DNA have rendered the development of our knowledge difficult. Investigation of complexes of DNA and synthetic nucleic acids with basic homopolypeptides poly(L-lysine) and poly(L-arginine) provides a greater simplicity and has been used by several groups of investigators employing different methods (Raukas, 1965; Tsuboi et al., 1966; Leng and Felsenfeld, 1966; Olins et al., 1967, 1968; Cohen and Kidson, 1968; Shapiro et al., 1969; Davidson and Fasman, 1969; Haynes et al., 1970; Caroll, 1972; Chang et al., 1973; Zama and Ishimura, 1973). Thermal denaturation studies showed that the formation of the complex with basic homopolypeptides leads to a substantial increase in the melting temperature which was interpreted as reflecting a marked stabilization of the double-helical structure of DNA (Olins et al., 1967, 1968; Inoue and Ando, 1970). The optical activity of DNA is drastically changed when it is complexed with these basic homopolypeptides. Thus, circular dichroism spectra of DNA covered by poly(L-lysine) are of inverted shape and nonconservative character; that is, a broad negative band is observed in the region of 280-240 nm, the intensity of which is greatly enhanced with respect to that of DNA (Haynes et al., 1970; Caroll, 1972).

Similar spectral changes were observed in DNA complexed with the histone f1 (Fasman et al., 1970; Adler et al., 1971). In contrast, complexes of arginine-rich histones f2a1 and also f2b with DNA exhibit circular dichroic (CD) spectra with increased amplitude of the 275-nm positive band (Shih and Fasman, 1971, 1972; Adler et al., 1974). The former spectral changes were considered as indicative of B → C transitions and the latter of B → A. Interpretations of spectral changes are very difficult since measurements of optical activity in these complexes may not only reflect the contribution of secondary structure. In fact, electron microscopy provides evidence that DNA-polylysine complexes and also f1-DNA and f2a1-DNA complexes form doughnut-shaped or globular particles with some internal periodicity (Haynes et al., 1970; Slayter et al., 1972). It is thus necessary to obtain structural information by another direct method, such as infrared linear dichroism (Bradbury et al., 1962). It was shown previously by Pilet and Brahms (1972, 1973) and Brahms et al. (1973) that precise structural parameters and structural transitions can be obtained from infrared linear dichroism studies of DNA. Unfortunately, previous X-ray diffraction investigations on DNA-poly(L-lysine) and DNA-poly(L-arginine) complexes cannot be considered here since they were performed under conditions

† From the Institut de Biologie moléculaire de la Faculte des Sciences de Paris, Paris 5ème, France, and the Uer de Médecine et Biologie Humaine, Université Paris XIII, 93000 Bobigny, France. *Received February 13, 1975.*

* Address correspondence to this author at the Institut de Biologie Moléculaire.